

See discussions, stats, and author profiles for this publication at: <https://www.researchgate.net/publication/231666961>

Artificial Muscle Reversibly Controlled by Enzyme Reactions

ARTICLE *in* JOURNAL OF PHYSICAL CHEMISTRY LETTERS · FEBRUARY 2010

Impact Factor: 7.46 · DOI: 10.1021/jz100070u

CITATIONS

23

READS

37

6 AUTHORS, INCLUDING:



Guinevere Strack

Air Force Civil Engineer Center

21 PUBLICATIONS 729 CITATIONS

[SEE PROFILE](#)



Mary Arugula

University of Wisconsin - Milwaukee

14 PUBLICATIONS 372 CITATIONS

[SEE PROFILE](#)



Marcos Pita

Spanish National Research Council

85 PUBLICATIONS 2,890 CITATIONS

[SEE PROFILE](#)



Jan Halánek

University at Albany, The State University of ...

79 PUBLICATIONS 1,729 CITATIONS

[SEE PROFILE](#)

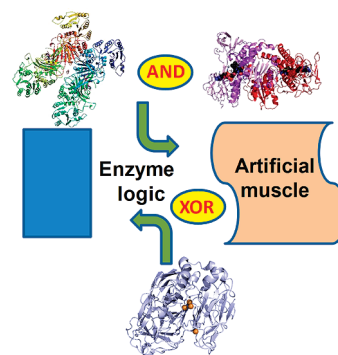
Artificial Muscle Reversibly Controlled by Enzyme Reactions

Guinevere Strack, Vera Bocharova, Mary A. Arugula, Marcos Pita, Jan Halámek, and Evgeny Katz*

Department of Chemistry and Biomolecular Science, and NanoBio Laboratory (NABLAB), Clarkson University, Potsdam, New York 13699-5810

ABSTRACT Chemically induced actuation of a polypyrrole (Ppy) artificial muscle was controlled by biocatalytic reactions, resulting in changes in the redox state of the polymer film mediated by soluble redox species. The biocatalytic process triggered by diaphorase in the presence of NADH resulting in the reduction of the Ppy film was reflected by the potential shift in the negative direction generated in the film. Conversely, the biocatalytic process driven by laccase in the presence of O_2 resulted in the oxidation of the Ppy film, thus yielding the positive potential shift. Both reactions produced opposite bending of the Ppy flexible strip, allowing reversible actuation controlled by the biocatalytic processes. The biocatalytic reactions governing the chemical actuator can be extended to multistep cascades processing various patterns of biochemical signals and mimicking logic networks. The present chemical actuator exemplifies the first mechanochemical device controlled by biochemical means with the possibility to scale up the complexity of the biochemical signal-processing system.

SECTION Macromolecules, Soft Matter



Conductive polymers,^{1,2} such as polypyrrole,³ polythiophene,⁴ and polyaniline,⁵ are frequently used for the modification of surfaces, providing control over interfacial properties that are dependent on the polymer matrix redox state. Electronic, optical, and mechanical properties of interfaces functionalized with conducting polymers can be reversibly switched/tuned by the variation of redox states in the polymeric matrices.¹ Redox changes in the conducting polymers result in the exchange of counterions between the polymer matrices and external solutions, thus resulting in the polymer films shrinking—swelling, allowing their application as artificial muscles.⁶ Coupling of the conducting polymers with flexible solid supports (e.g., macroscopic polymeric strips^{7–11} or microcantilevers^{12,13}) resulted in their mechanical bending upon reduction—oxidation of the polymer films. In most of the studies, the redox transformations of the conducting polymers resulting in the mechanical actuation were induced by electrochemical means, i.e., by applying an external potential to the conductive support functionalized with the polymer films.^{7–13} There are very few examples of chemically induced actuation triggered by redox transformations of the conducting polymers upon their reactions with reducing/oxidizing species applied in a solution.¹⁴ However, the importance of the actuation induced by chemical reactions cannot be overestimated; it is direct mechanical micro-manipulation controlled by biochemical means, which is an essential component of future implantable biomedical devices operating upon physiological commands. The present paper represents a novel approach to biochemical actuators

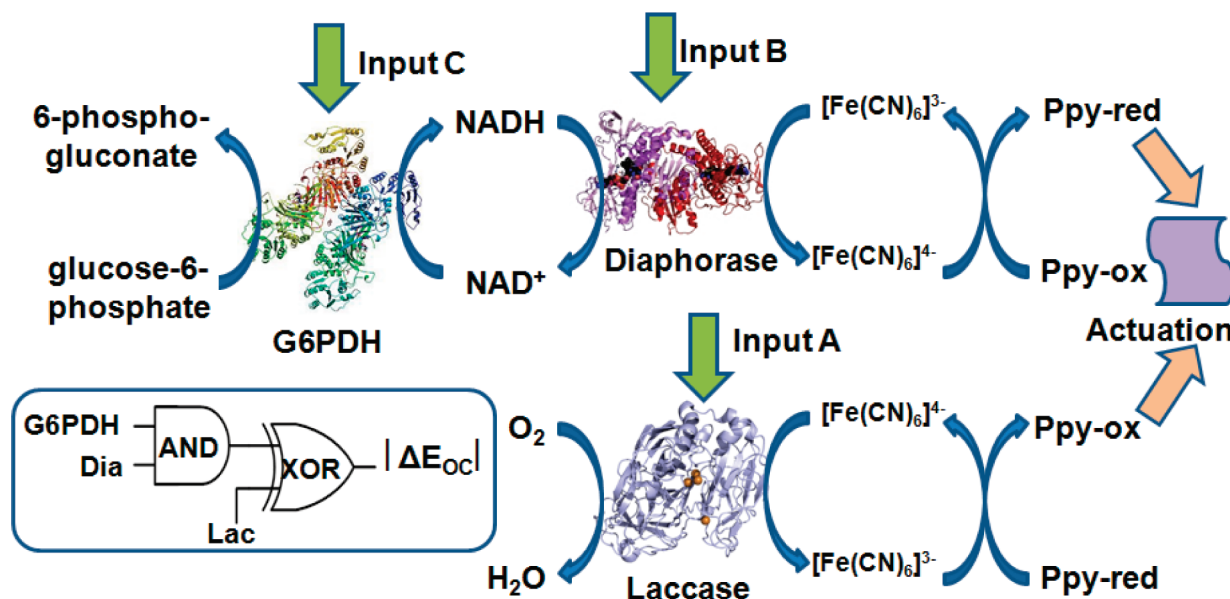
where the mechanical action performed by a conducting polymer is controlled by biochemical reactions and mediated by redox species governing the polymer redox state.

A 40-nm Au coating was sputtered on a polyimide (PI) tape of 25 μm thickness to yield a flexible electrode. A polypyrrole (Ppy) film was deposited on the electrode surface ($1 \times 20 \text{ mm}^2$ strip) by potentiostatic (+0.69 V vs $\text{Ag}|\text{AgCl}|\text{KCl}$, 3M) electropolymerization for 380 s from an aqueous solution composed of 0.2 M pyrrole and 0.2 M NaClO_4 following a standard procedure.¹⁵ After deposition, the Ppy film was conditioned in 0.5 M NaClO_4 by cycling at 150 mV s^{-1} from -650 mV to $+800 \text{ mV}$ until a stable cyclic voltammogram was achieved, followed by 1 h equilibration time to ensure consistent actuator performance. A cyclic voltammogram with a shape typical for a Ppy-modified electrode, $E_{1/2}$ ca. 0.05 V, pH 6.0, was obtained. The Ppy film average thickness of ca. 8.6 μm was estimated by electrochemical measurements. (The details of the electrode modification and characterization are given in the Supporting Information.) A solution containing a variable ratio of oxidized and reduced species, $[\text{Fe}(\text{CN})_6]^{3-}/[\text{Fe}(\text{CN})_6]^{4-}$ (total concentration of 10 mM in 0.5 M NaClO_4) was applied to vary the redox state of the Ppy film.¹⁴ Upon increasing the concentration of the reduced species, $[\text{Fe}(\text{CN})_6]^{4-}$, the conducting polymer was

Received Date: January 18, 2010

Accepted Date: February 1, 2010

Published on Web Date: February 11, 2010

Scheme 1. Biocatalytic Reactions Controlling the Chemical Actuator^a


^a Inset: Equivalent logic circuit corresponding to the input-processing biocatalytic cascade.

partially reduced, thus shifting the open circuit potential on the conducting support in the negative direction, while increasing the concentration of the oxidized species, $[\text{Fe}(\text{CN})_6]^{3-}$, resulted in the polymer oxidation moving the potential in the positive direction. The open circuit potential generated on the Ppy-modified electrode had a quasi-Nernstian dependence on the ratio of the soluble redox species, 47.6 mV per decade, similar to the value reported recently.¹⁴ The Ppy-modified strip demonstrated bending upon variation of the potential generated on it, originating from the redox induced volume change of the polymer film.

Two enzymes, laccase (Lac; from *Trametes versicolor*, E.C. 1.10.3.2) and diaphorase (Dia; from *Clostridium kluyveri*, E.C. 1.8.1.4), were applied to vary in situ the ratio of the redox-mediator species, $[\text{Fe}(\text{CN})_6]^{3-/4-}$, thus resulting in the biochemically controlled bending of the Ppy strip (Scheme 1). Laccase (Input A; 0.25 mg mL⁻¹) in the presence of oxygen oxidized $[\text{Fe}(\text{CN})_6]^{4-}$, which produced the oxidized state of the Ppy film and resulted in the positive shift of the potential generated on the Ppy strip. Diaphorase (Input B; 0.25 mg mL⁻¹) in the presence of NADH (12 mM) resulted in the reduction of $[\text{Fe}(\text{CN})_6]^{3-}$, thus producing the reduced state of the Ppy film and yielding the negative potential shift. The changes in the concentrations of the mediating redox species in the solution during the biocatalytic reactions were monitored by optical measurements at $\lambda = 420$ nm (absorbance maximum of $[\text{Fe}(\text{CN})_6]^{3-}$) (Figure 1, curve a). The shift of the open circuit potential generated on the Ppy strip was measured simultaneously (Figure 1, curve b). Both changes induced by the enzyme reactions proceeded in parallel with comparable rates. (Note that the concentration changes in Figure 1, curve a, are shown on the logarithmic scale to be compared with the potential shift according to the Nernst equation.) The redox changes induced by the enzymatic

reactions resulted in the macroscopic bending of the Ppy strip photographed using a digital camera (Figure 2a–c). In order to prove that the bending is controlled by the potential value chemically generated on the Ppy strip and that it is not dependent on the presence of specific chemicals, we applied an external potential on the Ppy strip in the absence of the biocatalytic and redox species in the solution. The external potential similar to the one chemically generated on the Ppy-strip resulted in the same bending of the strip (Figure 2d–f). Both methods, application of the external potential and the biocatalytic reactions, allowed reversible bending of the Ppy strip (Figure 3). It should be noted that the addition of the enzymes in the absence of the corresponding substrates (O_2 for laccase and NADH for diaphorase) did not result in any changes in the system. Similarly, the control experiment where NADH was added to or O_2 was removed from the solution did not affect the system in the absence of the enzymes.

In order to find the strain generated in the Ppy strip, the digital pictures of the curved strip at different applied or biochemically induced potentials (Figure 2) were converted to the numeric files using ImageJ free software, and the curvature, k , was calculated from the obtained data files using MATLAB software. The curvature was related to the Ppy strain, α_{Ppy} , using the Timoshenko equation, eq 1:¹⁶

$$\frac{1}{R} - \frac{1}{R_0} = k - k_0$$

$$= \frac{6(\alpha_{\text{Ppy}} - \alpha_{\text{Pi}})(1+m)^2}{h(3(1+m)^2 + (1+mn(m^2 + 1/mn)))} \quad (1)$$

where the radius, R , of the fitted circle was inversely proportional to the curvature, k ; R_0 and k_0 corresponded to the parameters measured at the resting potential. The two

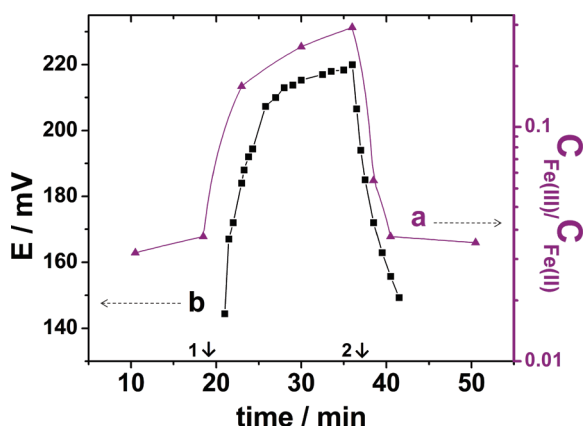


Figure 1. (a) Alteration of the redox states of the mediator species upon application of the enzyme signals. The concentrations of the reduced and oxidized species were derived from the absorbance measurements at $\lambda = 420$ nm. (b) The open circuit potential (vs Ag|AgCl|KCl, 3M) generated on the conductive support of the Ppy-functionalized strip upon the biochemical reactions. The reacting solution was composed of 10 mM $[\text{Fe}(\text{CN})_6]^{4-}$, 12 mM NADH, and O_2 (in equilibrium with air) in 0.5 M NaClO_4 aqueous solution, pH 6.0. The inputs included laccase (Input A; 0.25 mg mL^{-1}) and diaphorase (Input B; 0.25 mg mL^{-1}). Arrows 1 and 2 show the inject time for the enzyme signals A and B, respectively.

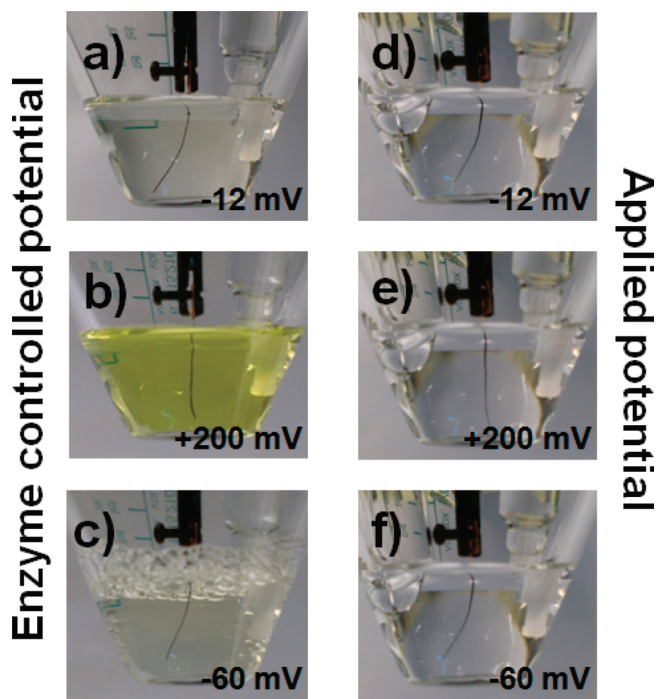


Figure 2. Images of the Ppy-functionalized strip upon application of various biochemical signals: (a) initial state of the strip before the signal application in the presence of 10 mM $\text{K}_4[\text{Fe}(\text{CN})_6]$ (note the initial reduced state of the redox mediator); (b) after the application of laccase (Input A; 0.25 mg mL^{-1}); (c) after application of diaphorase (Input B; 0.25 mg mL^{-1}). The reacting solution also included 12 mM NADH and O_2 (in equilibrium with air) in 0.5 M NaClO_4 aqueous solution, pH 6.0. Images of the Ppy-functionalized strip upon application of external electrical potentials: (d) -12 mV ; (e) $+200 \text{ mV}$; (f) -60 mV . The solution included only 0.5 M NaClO_4 . The digital images and the open circuit potential were obtained 180 s after the signal application.

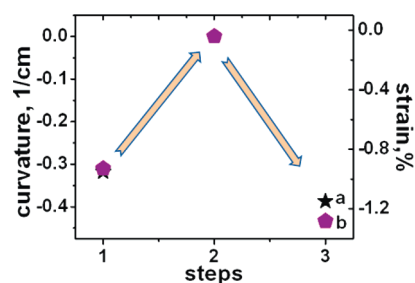


Figure 3. Reversible bending and strain generation in the Ppy-functionalized strip (a) after biochemical inputs of laccase (step 2) and diaphorase (step 3) and (b) upon application of external potentials of $+200 \text{ mV}$ (step 2) and -60 mV (step 3).

experimentally obtained values were the sum of the Ppy and PI layer thicknesses, $h = h_{\text{Ppy}} + h_{\text{PI}}$ ($h_{\text{Ppy}} = 8.6 \mu\text{m}$ and $h_{\text{PI}} = 25 \mu\text{m}$) and the curvature, $k = 1/R$. The remaining parameters were considered as the following relationships: $m = h_{\text{PI}}/h_{\text{Ppy}}$; $n = E_{\text{PI}}/E_{\text{Ppy}}$. The E moduli of the PI substrate and the Ppy film were represented as $E_{\text{PI}} = 2.9 \text{ GPa}$,¹⁴ $E_{\text{Ppy}} = 80 \text{ MPa}$ ^{14,17} respectively. The Au layer was not considered in this calculation due to the relatively small layer thickness of 40 nm. The relationship of the calculated strain to the measured curvature rests on the assumption that the bending of the Ppy actuator on the PI substrate is comparable to an actuator consisting of polymer only, which changes in length as a result of a change in the oxidative state. The reversible changes of the strain generated by an externally applied potential or biocatalytically produced through the redox mediator are also shown in Figure 3.

The biochemical reactions activated by the enzyme-signals resulting in the mechanical actuation of the Ppy-functionalized flexible strip can be considered as the information processing digital system and described in terms of logic operations.¹⁸ Since the biochemical inputs (laccase – signal A; diaphorase – signal B) yielded the opposite bending of the chemical actuator, their careful optimization resulted in the compensation of their effects, thus preserving the flexible strip in the resting position. If the output signal in the system is defined as an absolute value of the strip deflection from the resting position, the system mimicked the **XOR** logic operation with the logic output **1** obtained at the separate application of signals A or B, while their simultaneous application produced the logic output **0** upon their compensation.

The enzymatic reactions being directly responsible for the alteration of the Ppy redox state through the $[\text{Fe}(\text{CN})_6]^{3-/4-}$ redox mediator can be extended to multistep biocatalytic cascades activated by different enzymes and triggered by various biochemical inputs. In order to demonstrate this concept, we applied glucose-6-phosphate dehydrogenase (G6PDH; from *Leuconostoc mesenteroides*, E.C. 1.1.1.49) to generate NADH in situ in the presence of glucose-6-phosphate as a reducing agent. G6PDH (Input C; $14.7 \text{ units mL}^{-1}$) catalyzed reduction of NAD^+ (12 mM) in the presence of glucose-6-phosphate (20 mM), while the in situ produced NADH was consumed by diaphorase (Input B; 0.25 mg mL^{-1}) to yield the reduced redox mediator and to produce the corresponding bending of the Ppy-strip (Scheme 1). In this

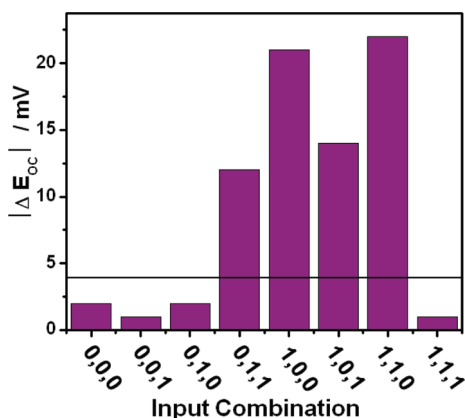


Figure 4. The bar chart showing the open circuit potential changes, $|\Delta E_{oc}|$, generated on the Ppy strip upon different combinations of the enzyme-input signals (A,B,C) corresponding to the three-enzyme biocatalytic system shown in Scheme 1. The system composition and the input concentrations are specified in the text. The line at $|\Delta E_{oc}| = 3.75$ mV corresponds to the threshold value separating 0 and 1 logic output signals generated in the system.

example the Ppy-strip bending was triggered by the two-step biocatalytic reaction. Careful optimization of the biocatalytic cascade allowed Ppy-strip bending comparable with that obtained upon direct addition of NADH concentrations similar to those of the solution containing diaphorase as described above. It should be noted that the final result (the Ppy-strip bending) can be achieved only upon completion of both steps in the biocatalytic cascade. Therefore, this system could mimic the logic operation **AND** when the application of both biochemical signals (diaphorase – Input **B**; G6PDH – Input **C**) resulted in the logic output **1** (bending of the actuator from its resting position), while the separate application of the biochemical signals did not produce the strip bending, resulting in the logic output **0**.

The complex system controlled by all three biochemical inputs can be represented by a logic network composed of **AND–XOR** concatenated logic gates (Scheme 1, inset). The three-input logic system was constructed in the presence of a 1:9 ratio of $[\text{Fe}(\text{CN})_6]^{3-}:[\text{Fe}(\text{CN})_6]^{4-}$ and optimized with 12 mM NAD^+ , 0.04 mg mL^{-1} of diaphorase (Input **B**) and 0.8 mg mL^{-1} of laccase (Input **A**). NADH was produced in situ in the presence of 12 mM NAD^+ , 20 mM glucose-6-phosphate, and 14.7 units mL^{-1} of G6PDH (Input **C**). When both Inputs **B** and **C** were present, the in situ produced NADH resulted in the biocatalytic transfer of electrons to $[\text{Fe}(\text{CN})_6]^{3-}$ yielding a decrease of the open circuit potential and the corresponding bending of the Ppy strip. The individual addition of Input **B** or Input **C** to the reaction solution did not result in a change in the open circuit potential, thus, only the combination of the two inputs induced a change in the measured potential and the strip bending. The application of laccase (Input **A**) resulted in the opposite process in the system. The performance of the enzyme-activated actuator was characterized by measuring the open circuit potential change $|\Delta E_{oc}|$, in the presence of specific input combinations (Figure 4). It should be noted that the potential change was directly related to the mechanical bending of the Ppy strip, thus allowing the use of $|\Delta E_{oc}|$ as the output signal of the system. The experimental results shown

Table 1. The Truth Table Showing the Output Signal Generated upon Application of Various Combinations of the Enzyme Inputs

Input A (Lac)	Input B (Dia)	Input C (G6PDH)	Output $ \Delta E_{oc} $
0	0	0	0
0	0	1	0
0	1	0	0
0	1	1	1
1	0	0	1
1	0	1	1
1	1	0	1
1	1	1	0

in Figure 4 correspond to the truth table, Table 1, expected for the network composed of the **AND–XOR** concatenated logic gates.

The biochemical reactions used in the present study to induce the actuator function could be further scaled up in their complexity using the recently developed approach for information processing by enzyme reactions,¹⁸ thus potentially allowing the actuator operation controlled by numerous signals logically processed by biochemical networks. The present concept of the “smart” logically controlled actuator will find important applications in implantable biomedical devices.¹⁹ For example, artificial microvalves, regulating biological fluids, and drug release controlled by physiological inputs will be among the most important applications. Miniaturization of the actuators controlled by biological signals to micro- and even nanoscale is feasible.²⁰

Recent advances in biomolecular information processing,¹⁸ specifically in enzyme-based logic gates²¹ and networks,²² already allowed processing of multiple biochemical signals and the use of the logically generated outputs to control nanostructured materials²³ and interfaces.²⁴ Biocatalytic electrodes,²⁵ biofuel cells,²⁶ and membranes²⁷ were switched between different states produced upon their interaction with biocatalytic cascades processing biochemical signals. The present work represents another facet of our multidisciplinary research area and opens the way for designing chemical actuators performing mechanical functions while being controlled by different patterns of biochemical signals logically processed by enzyme networks. Microrobotic and bioimplantable devices²⁸ are among the most likely applications to benefit from advances in biochemical information processing coupled with mechano-chemical actuation. Future progress in these areas will depend on the development of novel computing concepts²⁹ and the design of new signal-responsive and information processing materials²³ as well as their integration with biochemically controlled microelectromechanical systems (MEMS).

SUPPORTING INFORMATION AVAILABLE Experimental procedure as well as Ppy-strip preparation and characterization. This material is available free of charge via the Internet at <http://pubs.acs.org>.

AUTHOR INFORMATION

Corresponding Author:

*To whom correspondence should be addressed. E-mail: ekatz@clarkson.edu.

ACKNOWLEDGMENT This research was supported by the National Science Foundation (Grant DMR-0706209), by the ARO (Grant W911NF-05-1-0339), by ONR (Grant N00014-08-1-1202) and by the Semiconductor Research Corporation (Award 2008-RJ-1839G). G.S. acknowledges the Wallace H. Coulter scholarship from Clarkson University.

REFERENCES

- Inzelt, G. *Conducting Polymers*; Springer: Berlin/Heidelberg, 2008.
- Handbook of Conducting Polymers*; Skotheim, T. A., Elsenbaumer, R. L., Reynolds, J. R., Eds.; Marcel Dekker, Inc.: New York, 1998.
- Wang, L.-X.; Li, X.-G.; Yang, Y.-L. Preparation, Properties and Applications of Polypyrroles. *React. Funct. Polym.* **2001**, *47*, 125–139.
- Schopf, G.; Kossmehl, G. *Polythiophenes: Electrically Conductive Polymers*; Springer: Berlin, 1997.
- Kang, E. T.; Neoh, K. G.; Tan, K. L. Polyaniline, A Polymer with Many Interesting Intrinsic Redox States. *Prog. Polym. Sci.* **1998**, *23*, 277–324.
- Baughman, R. H. Conducting Polymer Artificial Muscles. *Synth. Met.* **1996**, *78*, 339–353.
- Otero, T. F.; Sansiñena, J. M. Bilayer Dimensions and Movement in Artificial Muscles. *Bioelectrochem. Bioenerg.* **1997**, *42*, 117–122.
- Otero, T. F.; Sansiñena, J. M. Artificial Muscles Based on Conducting Polymers. *Bioelectrochem. Bioenerg.* **1995**, *38*, 411–414.
- Otero, T. F.; Sansiñena, J. M. Soft and Wet Conducting Polymers for Artificial Muscles. *Adv. Mater.* **1998**, *10*, 491–494.
- Takashima, W.; Kaneko, M.; Kaneto, K.; MacDiarmid, A. G. The Electrochemical Actuator Using Electrochemically-Deposited Polyaniline Film. *Synth. Met.* **1995**, *71*, 2265–2266.
- Qibing, P.; Inganlås, O. Conjugated Polymers and the Bending Cantilever Method: Electrical Muscles and Smart Devices. *Adv. Mater.* **1992**, *4*, 277–278.
- Smela, E.; Inganas, O.; Lundstrom, I. Controlled Folding of Micrometer-Size Structures. *Science* **1995**, *268*, 1735–1738.
- Lahav, M.; Durkan, C.; Gabai, R.; Katz, E.; Willner, I.; Welland, M. E. Redox Activation of a Polyaniline-Coated Cantilever: An Electro-Driven Microdevice. *Angew. Chem., Int. Ed.* **2001**, *40*, 4095–4097.
- Küttel, C.; Stemmer, A.; Wei, X. Strain Response of Polypyrrole Actuators Induced by Redox Agents in Solution. *Sens. Actuat. B* **2009**, *141*, 478–484.
- Sadki, S.; Schottland, P.; Brodie, N.; Sabouraud, G. The Mechanisms of Pyrrole Electropolymerization. *Chem. Soc. Rev.* **2000**, *29*, 283–293.
- Timoshenko, S. P.; Goodier, J. N. *Theory of Elasticity*, 3rd ed; McGraw-Hill International Editions, 1970.
- Otero, T. F.; Cascales, J. J. L.; Arenas, G. V. Mechanical Characterization of Free-Standing Polypyrrole Film. *Mater. Sci. Eng., C* **2007**, *27*, 18–22.
- Katz, E.; Privman, V. Enzyme-Based Logic Systems for Information Processing. *Chem. Soc. Rev.* [Online early access]. DOI:10.1039/B806038J.
- Smela, E. Conjugated Polymer Actuators for Biomedical Applications. *Adv. Mater.* **2003**, *15*, 481–494.
- Pedrosa, V. A.; Luo, X.; Burdick, J.; Wang, J. "Nanofingers" Based on Binary Gold–Polypyrrole Nanowires. *Small* **2008**, *4*, 738–741.
- Zhou, J.; Arugula, M. A.; Halámek, J.; Pita, M.; Katz, E. Enzyme-Based NAND and NOR Logic Gates with Modular Design. *J. Phys. Chem. B* **2009**, *113*, 16065–16070.
- Privman, V.; Arugula, M. A.; Halámek, J.; Pita, M.; Katz, E. Network Analysis of Biochemical Logic for Noise Reduction and Stability: A System of Three Coupled Enzymatic AND Gates. *J. Phys. Chem. B* **2009**, *113*, 5301–5310.
- Pita, M.; Minko, S.; Katz, E. Enzyme-Based Logic Systems and Their Applications for Novel Multi-Signal-Responsive Materials. *J. Mater. Sci.: Materials in Medicine* **2009**, *20*, 457–462.
- Privman, M.; Tam, T. K.; Pita, M.; Katz, E. Switchable Electrode Controlled by Enzyme Logic Network System: Approaching Physiologically Regulated Bioelectronics. *J. Am. Chem. Soc.* **2009**, *131*, 1314–1321.
- Zhou, J.; Tam, T. K.; Pita, M.; Ornatska, M.; Minko, S.; Katz, E. Bioelectrocatalytic System Coupled with Enzyme-Based Bio-computing Ensembles Performing Boolean Logic Operations: Approaching "Smart" Physiologically Controlled Biointerfaces. *ACS Appl. Mater. Interfaces* **2009**, *1*, 144–149.
- Katz, E.; Pita, M. Biofuel Cells Controlled by Logically Processed Biochemical Signals: Towards Physiologically Regulated Bioelectronic Devices. *Chem.—Eur. J.* **2009**, *15*, 12554–12564.
- Tokarev, I.; Gopishetty, V.; Zhou, J.; Pita, M.; Motornov, M.; Katz, E.; Minko, S. Stimuli-Responsive Hydrogel Membranes Coupled with Biocatalytic Processes. *ACS Appl. Mater. Interfaces* **2009**, *1*, 532–536.
- Tsuda, S.; Zauner, K.-P.; Gunji, Y.-P. Robot Control with Biological Cells. *Biosystems* **2007**, *87*, 215–223.
- Zauner, K. P. Molecular Information Technology. *Crit. Rev. Solid State Mater. Sci.* **2005**, *30*, 33–69.